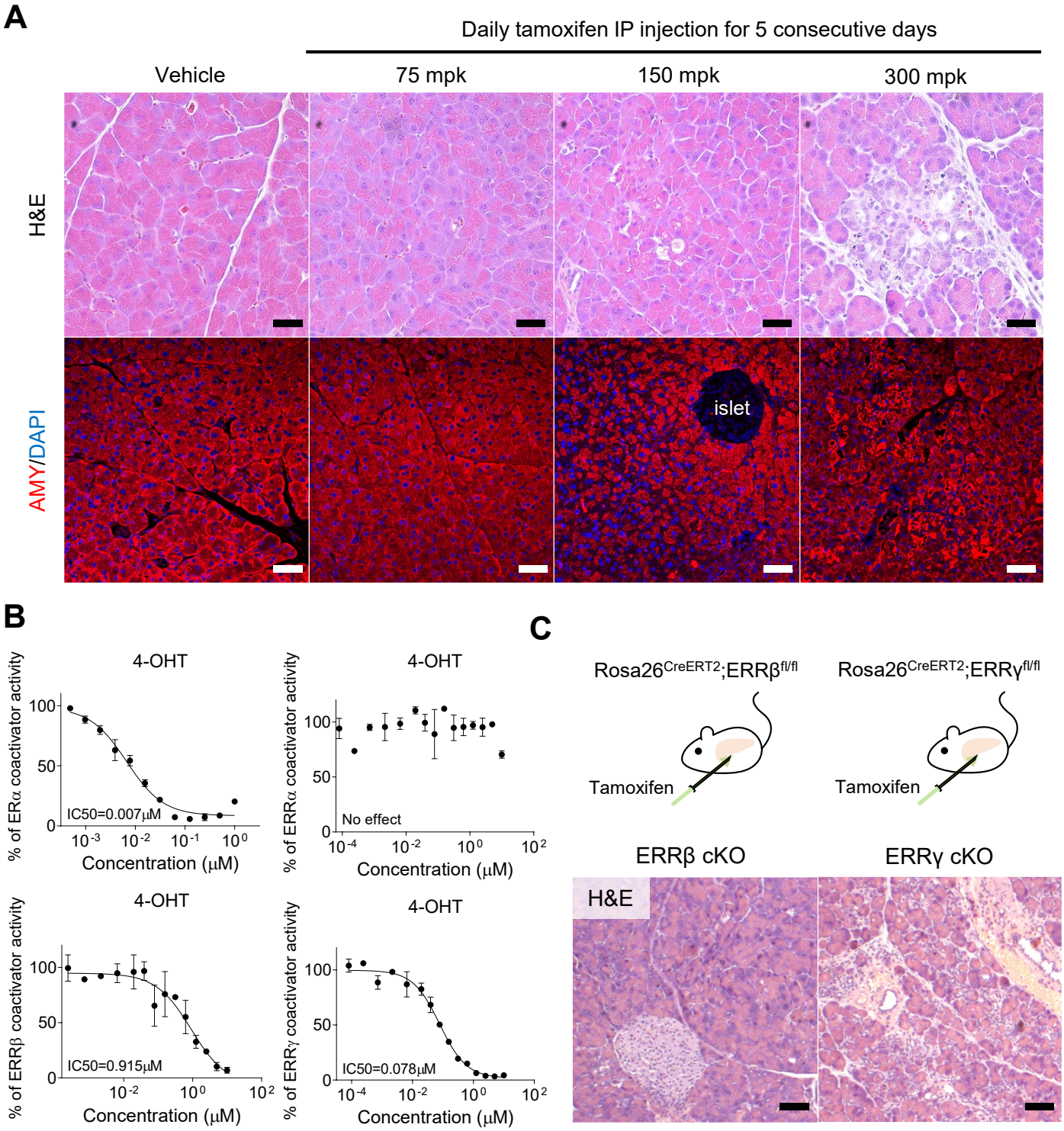

Supplementary Figure 1. Tamoxifen induces exocrine pancreas damage in a dose-dependent manner and inhibits ERRγ-coactivator.

(A) H&E and immunofluorescence images from pancreas tissue. TAM was intraperitoneally injected daily for 5 consecutive days at the indicated dose. mpk, mg TAM/ kg body weight; AMY, amylase; DAPI, nucleus. Scale bar, 50 μm. (B) 4-OHT, 4-hydroxytamoxifen, binding assay for ERRs and ERα was performed using Lanthascreen assay system (Life Technologies, Grand Island, NY, USA), which was based on TR-FRET, following manufacturer's instruction. The binding activity in the presence of compounds was represented as the percentage of control binding activity, and the IC_{50} value was calculated with non-linear regression fit with four parameters using the Prism 8.3 software. All IC_{50} values were statistically evaluated by R-squared value of goodness-of-fit, which was over 0.9. (C) R26-CreERT2; ERRβ$^{fl/fl}$ and R26-CreERT2; ERRγ$^{fl/fl}$ mice were generated. H&E images of pancreas tissue from mice at 1 d after the final TAM injection. Scale bar, 50 μm. All data are presented as mean ± SEM.

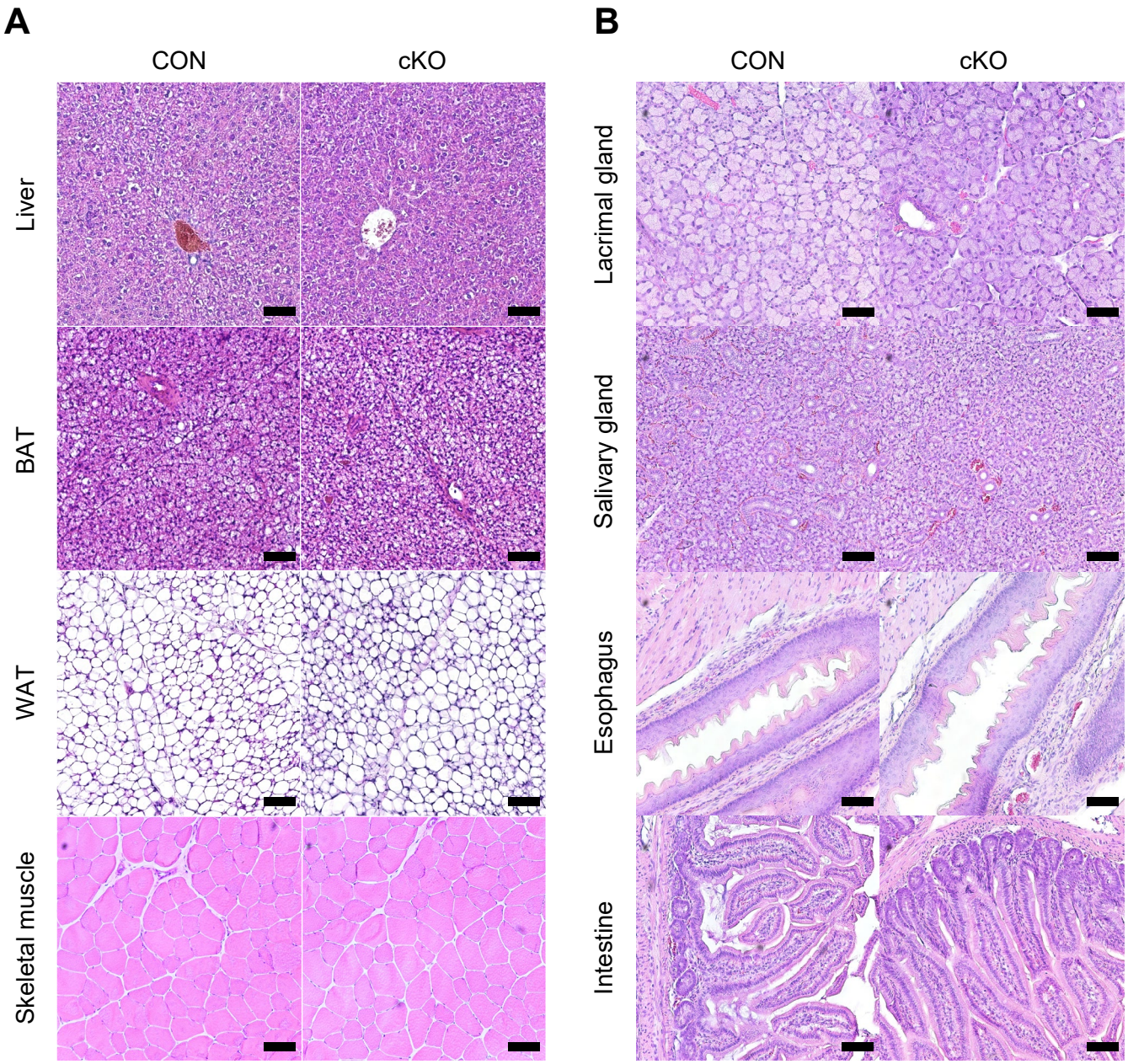

Supplementary Figure 2. ERRγ cKO mice do not display apparent phenotypes in non-pancreatic tissues.

(A) H&E staining from metabolic tissues including liver, brown adipose tissue (BAT) and white adipose tissue (WAT) and skeletal muscle. (B) H&E staining from various glands including lacrimal gland, salivary gland, esophagus, and intestine. Tissues were obtained from male control (CON) and ERRγ cKO (cKO) mice at d 7 after the final TAM injection. Scale bar, 50 μm.

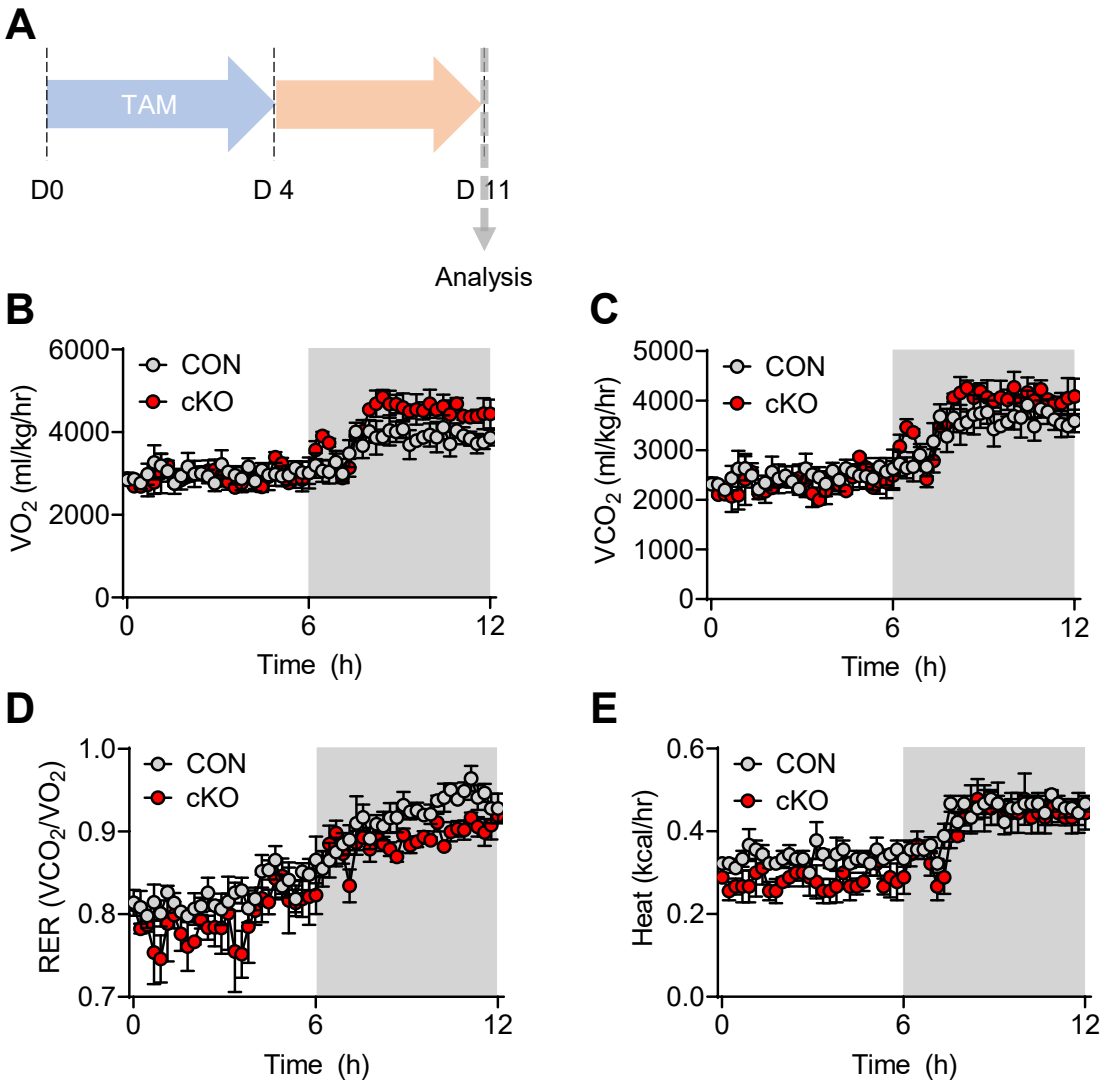

Supplementary Figure 3. ERRγ cKO mice do not display alterations in energy expenditure and respiratory exchange ratio.

(A) Scheme of experimental design. Mice were intraperitoneally injected with tamoxifen (75 mg/kg) once daily for 5 consecutive days (d 0 ~ d 4) and then housed in metabolic chambers for 72 h at d 11. (B-E) Measurement of (B) oxygen consumption (VO_2), (C) carbon dioxide production (VCO_2), (C) respiratory exchange ratio (RER), and (D) heat production in control during light (no shade) and dark (gray shade) cycles. CON, control (n = 3, male); cKO, ERRγ cKO (n = 3, male). All data presented as mean ± SEM.

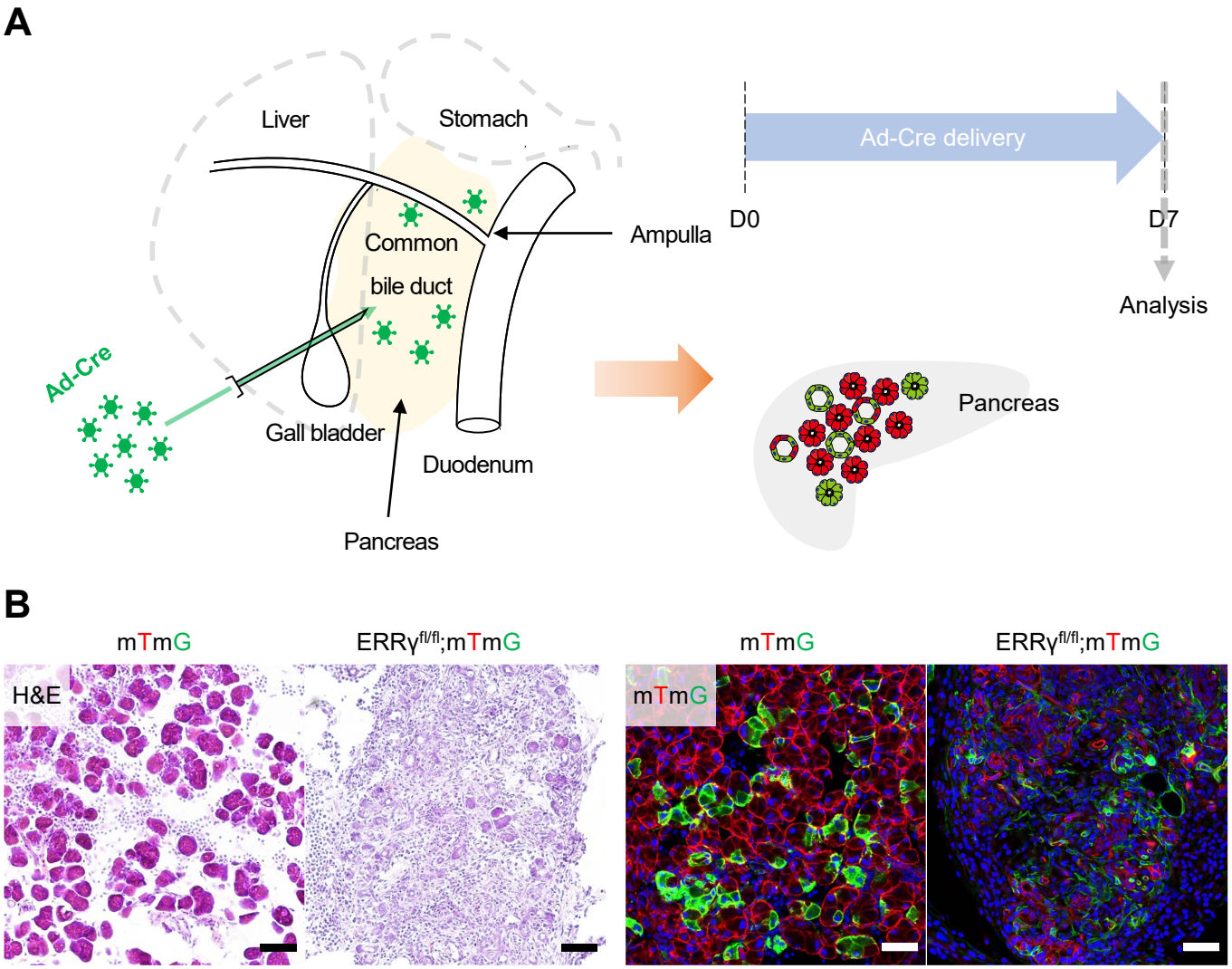

Supplementary Figure 4. Local ERRγ deletion in the pancreas is sufficient to induce pancreatic degeneration.

(A) Scheme of experimental design. Pancreatic parenchyma of control (mTmG) and ERRγ$^{fl/fl}$; mTmG mice were injected with adenovirus expressing Cre recombinase (Ad-Cre). In the mTmG reporter mice, all cells express membrane-targeted tdTomato (mT) prior to Cre expression, whereas the Cre-expressing cells express membrane-targeted GFP (mG). Mice were analyzed 7 d after Ad-CRE injection. (B) H&E staining (left panel) and fluorescence images (right panel) from frozen pancreas sections. Green fluorescence indicates Ad-Cre-mediated recombination. Scale bar, 50 μm.

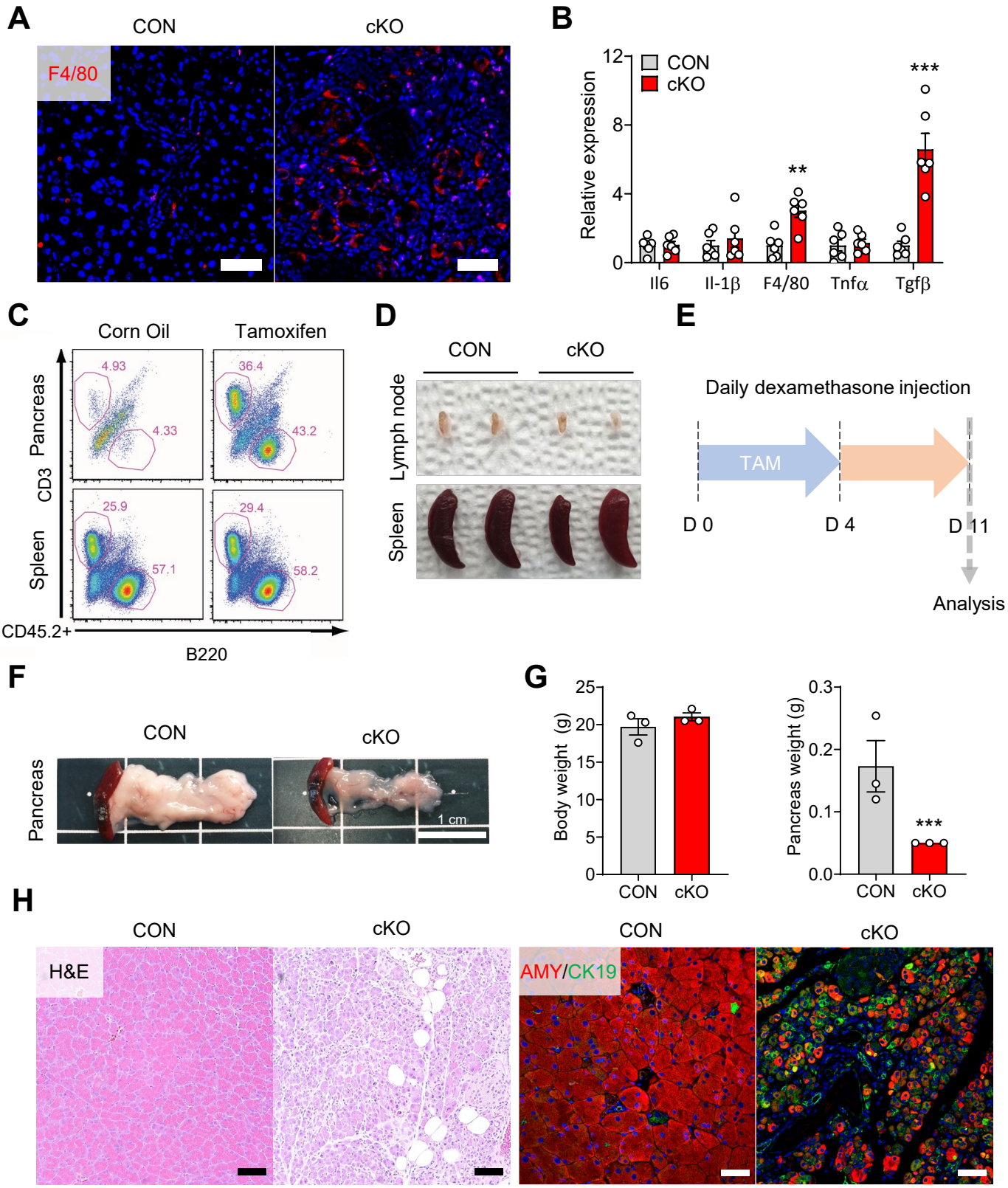

Supplementary Figure 5. ERRγ cKO pancreas displays local inflammation and immune cell infiltration.

(A) Immunofluorescence images of F4/80 (red) and DAPI (blue). Scale bar, 50 μm. (B) qPCR analysis of inflammatory cytokine gene expression from control and ERRγ cKO pancreas at 4 d after the last TAM injection. (C) CD4 or CD8 positive cell population in pancreas and spleen. (E) Scheme of experimental design. Mice were intraperitoneally injected with dexamethasone (5 mg/kg) daily throughout the experiment (d 0 ~ d 11). TAM (75 mg/kg) was administered once daily by oral gavage for 5 consecutive days (d 0 ~ d 4) and mice were sacrificed and analyzed 7 d after final TAM treatment. (F) Gross images of pancreas tissue attached to spleen. Scale bar, 1cm. (G) body weights and pancreas weights. (H) H&E images (left panel) and immunofluorescence images (right panel) for amylase (AMY, red) and DAPI (blue) of control and ERRγ cKO mice pancreas. CON, control; cKO, ERRγ cKO. Scale bar, 50 μm. All data are presented as mean ± SEM. ** $p < 0.01$, *** $p < 0.005$, by student's t-test.

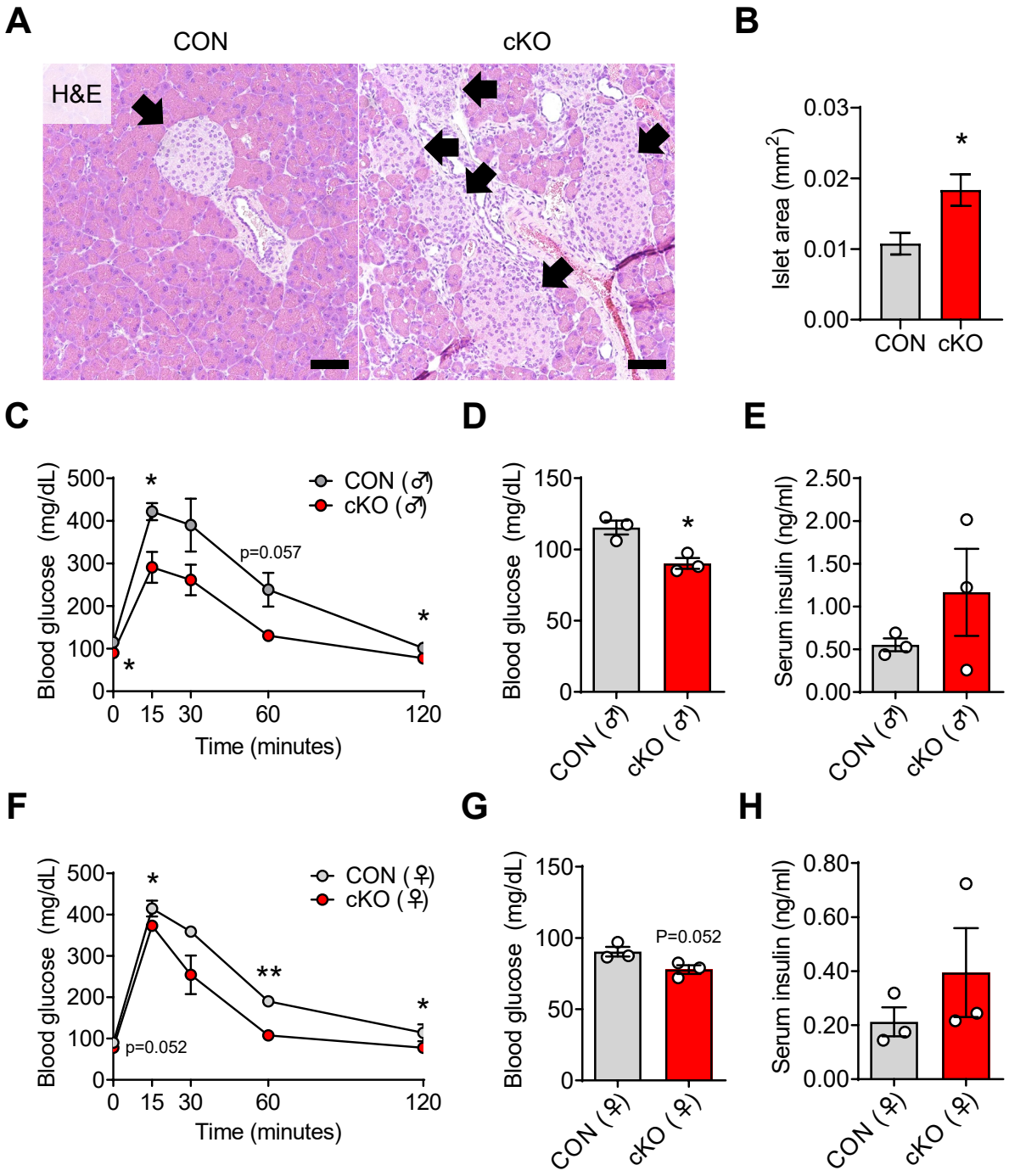

Supplementary Figure 6. ERRγ cKO mice exhibit islet hypertrophy and increased glucose tolerance.

(A) H&E staining of pancreas from control and ERRγ cKO mice at d 7 after the final TAM injection. (B) Measurement of islet area in control and ERRγ cKO mice. (C-E) Measurement of glucose tolerance test (C), fasting blood glucose (D), and random serum insulin (E) in control and ERRγ cKO male mice. (F-H) Measurement of glucose tolerance test (F), fasting blood glucose (G), and random serum insulin (H) in control and ERRγ cKO female mice. CON, control; cKO, ERRγ cKO. All data presented as mean ± SEM. * $p < 0.05$, ** $p < 0.01$ by student's t-test.

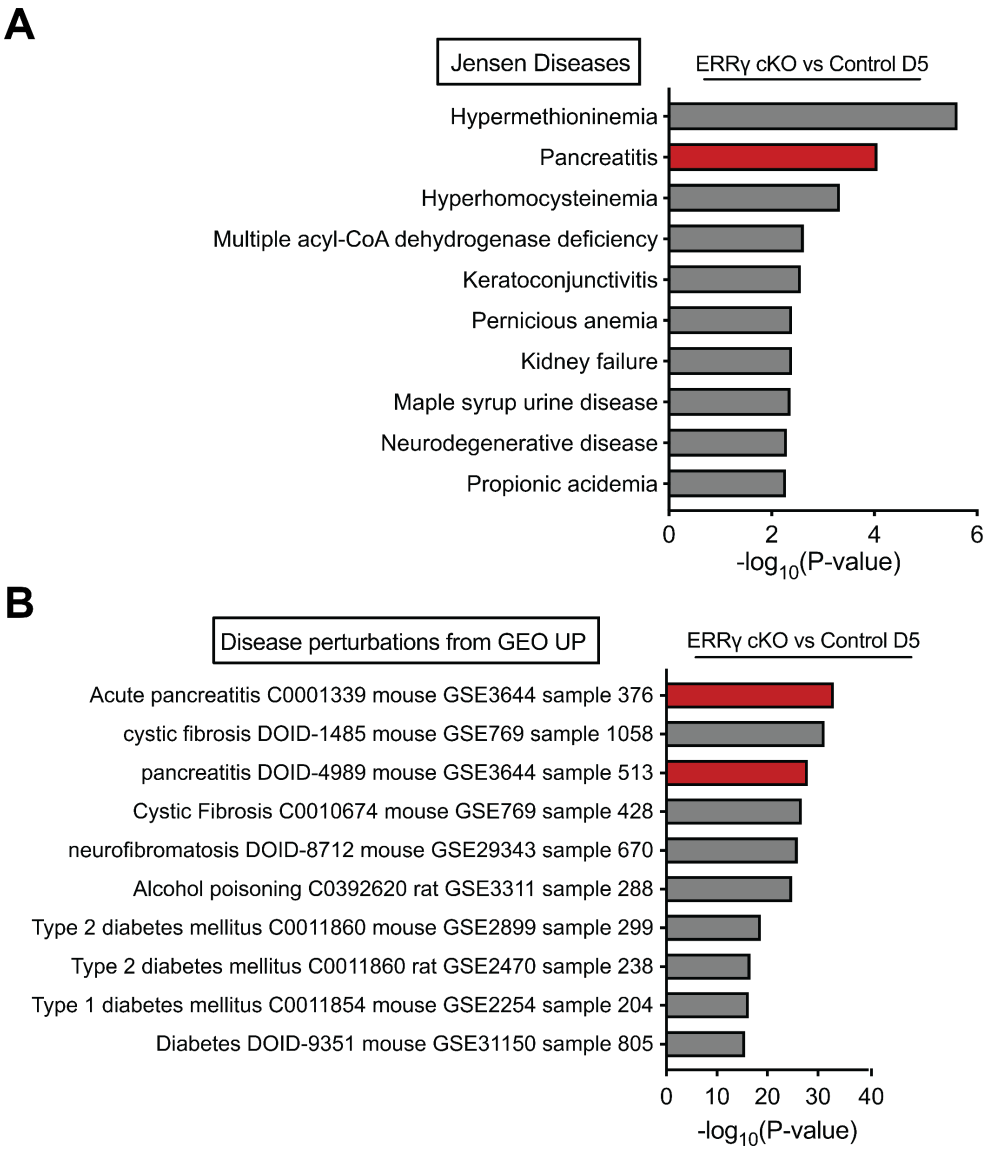

Supplementary Figure 7. ERRγ cKO pancreas RNA-seq data correspond to human pancreatitis gene expression signatures.

(A) Enrichr analysis predicts diseases using the Jensen database. The down-regulated set from mouse RNA-seq is associated with pancreatitis. The scale was presented in $-\log_{10}$(P-value). (B) Enrichr analysis predicts diseases using the Disease perturbation from GEO UP. The down-regulated set from mouse RNA-seq is associated with acute pancreatitis of the previous studies. The scale was presented in $-\log_{10}$(P-value).

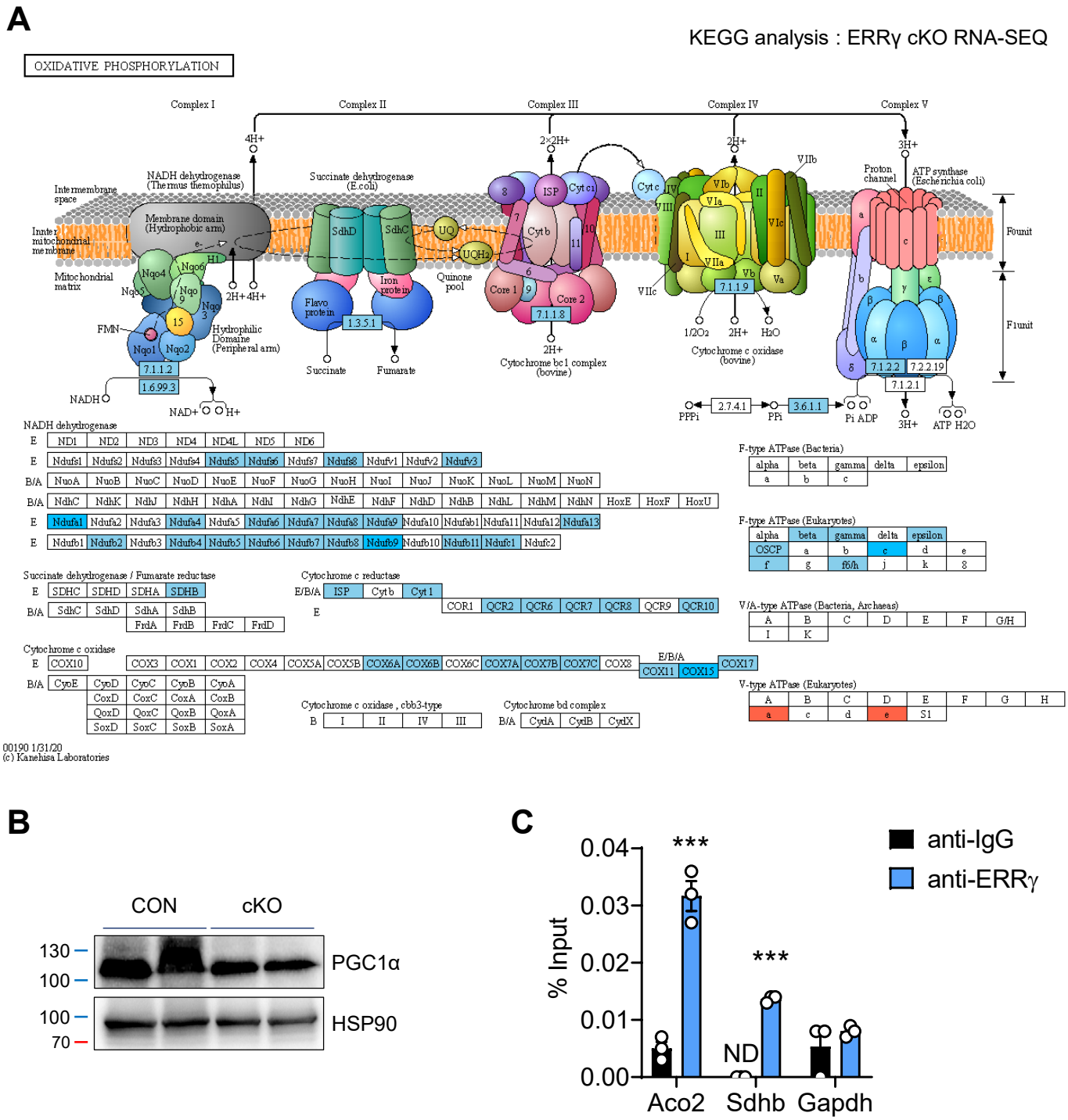

Supplementary Figure 8. Mitochondrial OXPHOS complex gene expression is downregulated in ERRγ cKO pancreas.

(A) KEGG pathway analysis for OXPHOS genes in RNA-seq data from primary acini isolated from ERRγ cKO mice 4 d after the final TAM injection. Blue-shaded boxes indicate downregulated genes, while red-shaded boxes indicate upregulated genes compared to control. (B) PGC1α with internal control, HSP90 4 d after the final TAM injection. (C) ChIP-qPCR assay using mouse primary acini from male C57BL6/J mice indicates enrichment of ERRγ occupancy at mitochondrial genes Aco2 and Sdhb. Data presented as mean ± SEM. *** $p < 0.005$, by student's t-test.

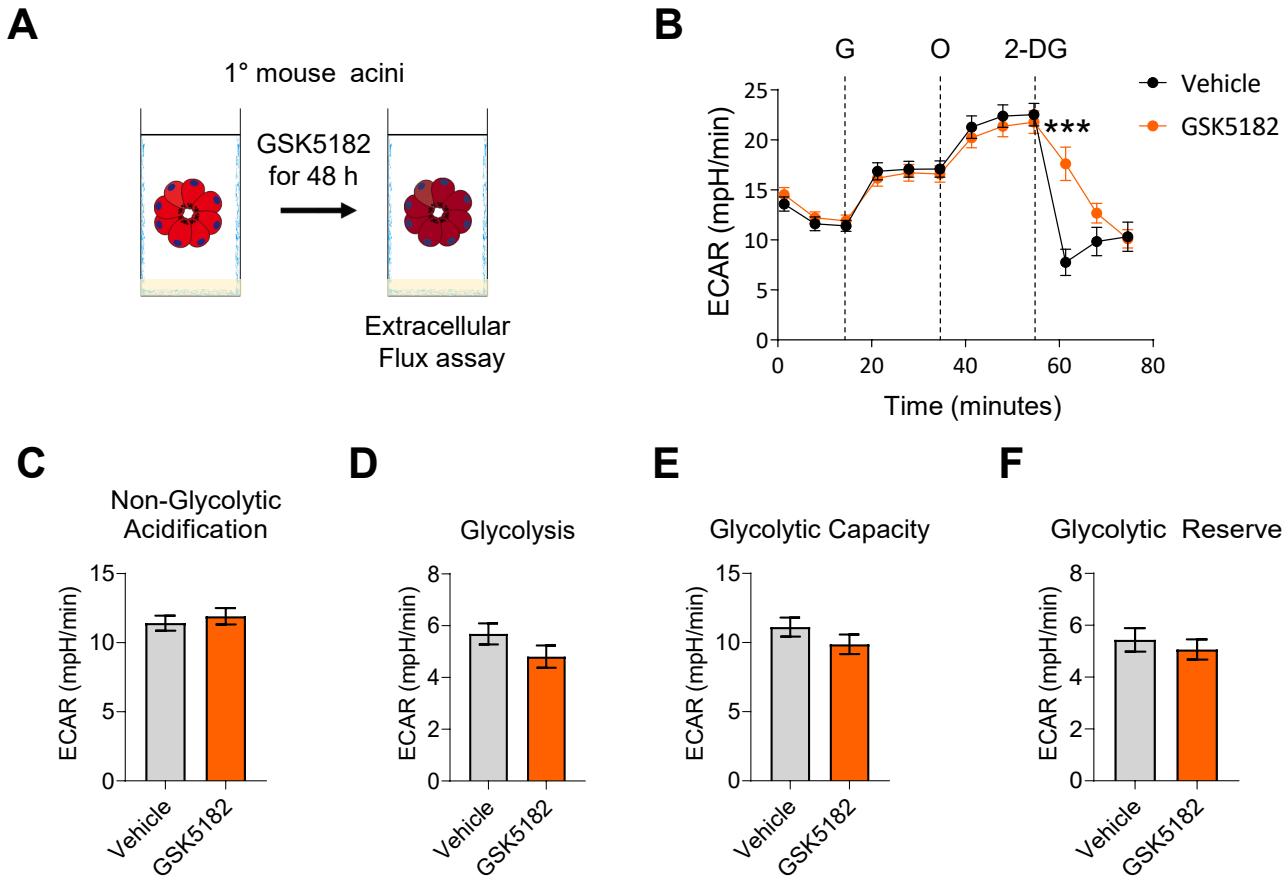

Supplementary Figure 9. Pharmacological inhibition of ERRγ does not affect glycolysis in primary acini.

(A) Scheme of experiments. Primary acini from C57BL/6J mice were treated with vehicle or GSK5182 (10 μM) for 48 h. (B-F) Extracellular flux analysis measurements for (B) extracellular acidification rate (ECAR), (C) non-glycolytic acidification, ECAR contributed by TCA cycle CO_2 evolution, (D) glycolysis, ECAR induced by glucose, (E) glycolytic capacity, ECAR induced by oligomycin treatment, and (F) glycolytic reserve, ECAR difference between glycolysis and glycolytic capacity. G, glucose; O, oligomycin; 2-DG, 2-deoxyglucose. n=44 per group. All data are presented as mean ± SEM. *** $p < 0.005$ by two-way ANOVA.

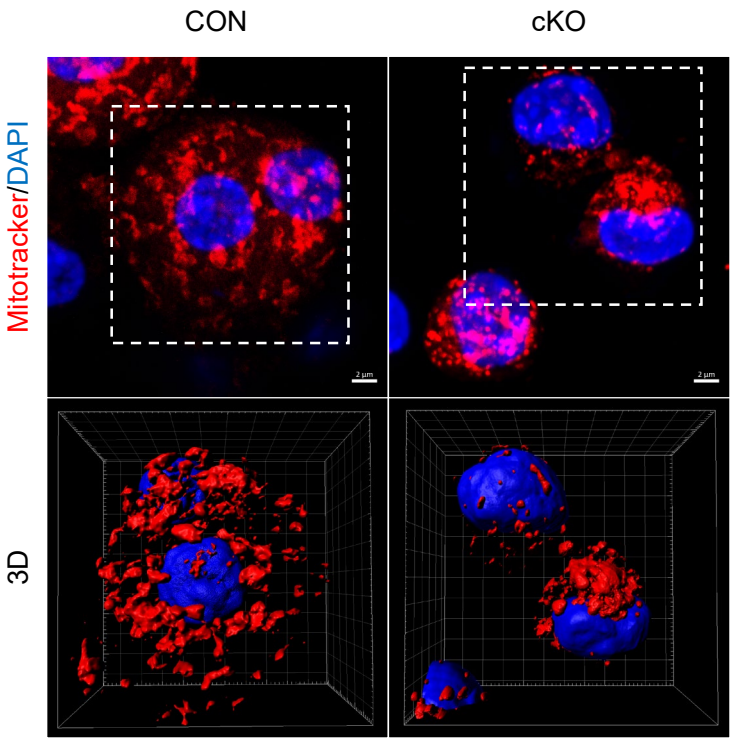

Supplementary Figure 10. ERRγ deletion leads to perinuclear accumulation of mitochondria.

Primary acini stained with mitotracker (red) and DAPI (blue). 3D surface image reconstruction was generated using Imaris software. CON, control; cKO, ERRγ cKO. Scale bar, 2 μm.

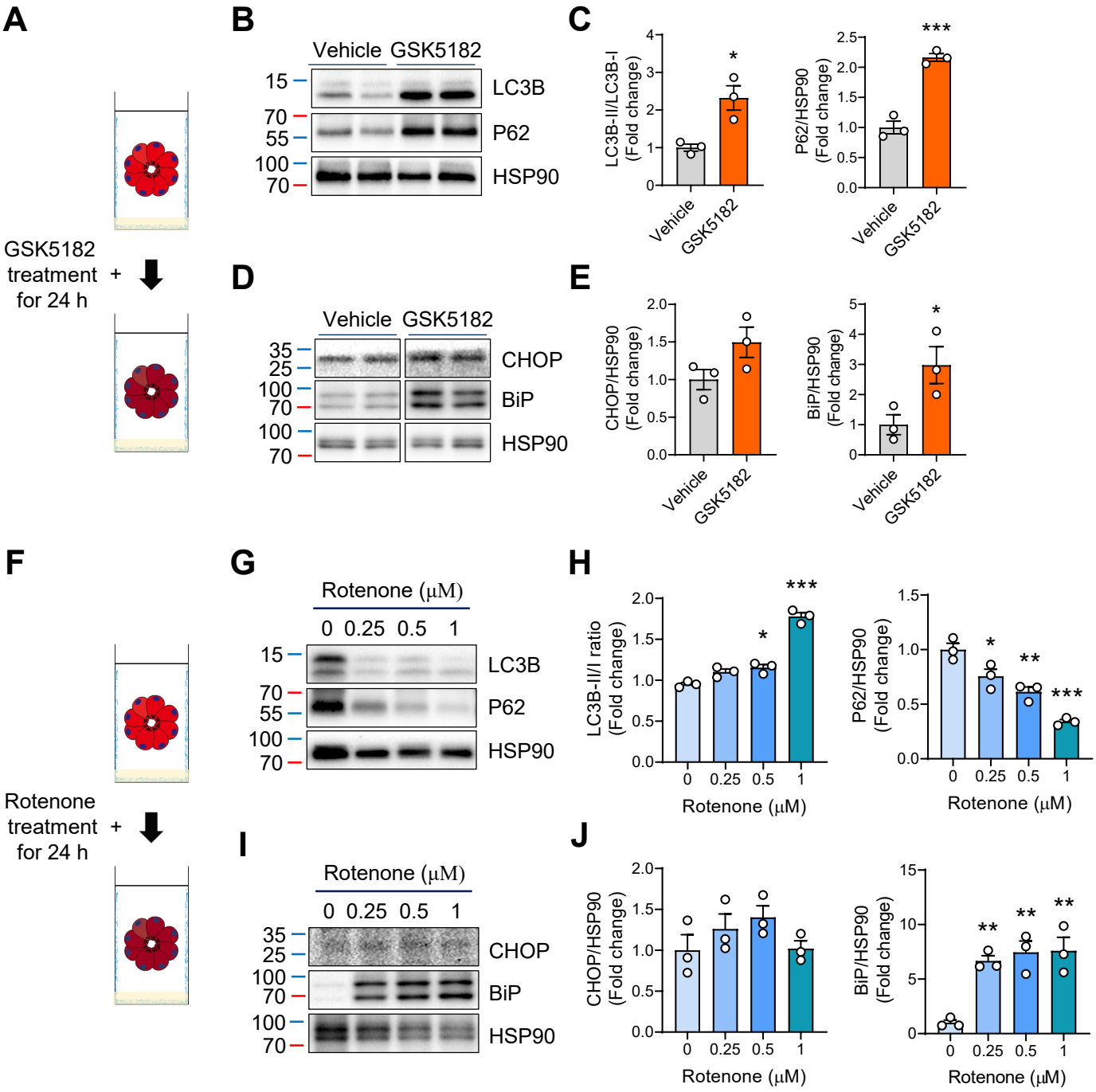

Supplementary Figure 11. ERRγ inverse agonist and mitochondrial complex I inhibitors induce autophagy and ER stress in primary acini.

(A) Scheme of experimental design. Mouse primary acini were treated with GSK5182 10 μM for 24 h. (B and D) Western blot for autophagy markers (B) and ER stress markers (D). (C and E) Quantitation of autophagy markers (C) and ER stress markers (E). Protein expression was normalized to HSP90. (F) Scheme of experimental design. Mouse primary acini were incubated with 0, 0.25, 0.5 and 1 μM rotenone for 24 h. (G and I) Western blot for autophagy markers (G) and ER stress markers (I). (H and J) Quantitation of autophagy markers (H) and ER stress markers (J). All data are presented as mean ± SEM. * $p < 0.05$, *** $p < 0.005$, by student's t-test.

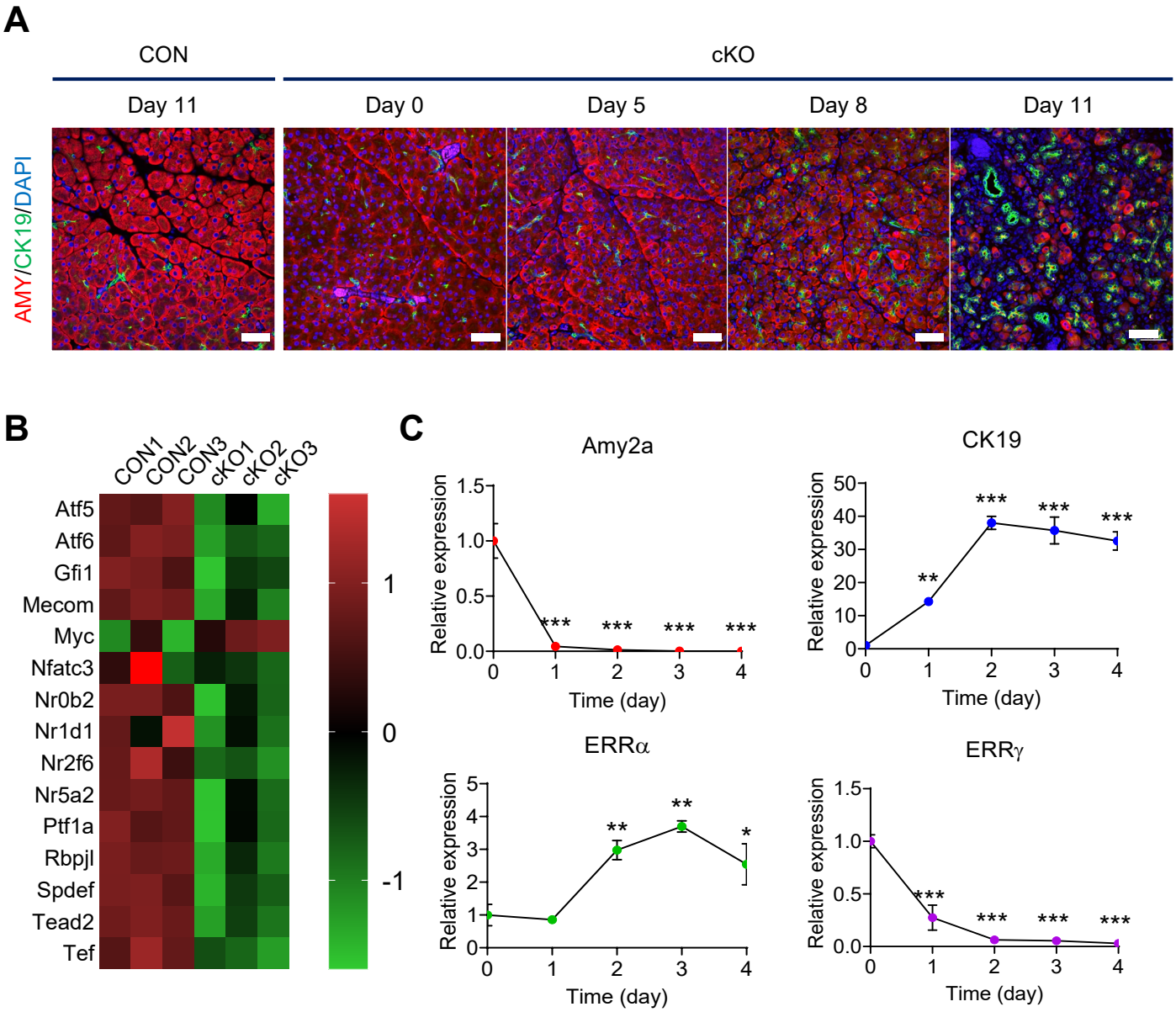

Supplementary Figure 12. ERRγ deletion induces acinar to ductal transdifferentiation.

(A) Images of control and ERRγ cKO mice pancreas sections with fluorescence immunostaining for amylase (AMY, red), cytokeratin19 (CK19, green), and DAPI (blue). Scale bar, 50 μm. Analysis performed on pancreas from indicated day after final TAM injection (B) Heatmap of genes regulating acinar cell identity from RNA-seq analysis of primary acini from control and ERRγ KO mice 4 d after the final TAM injection. (C) Gene expression analysis of primary acini cultured in matrigel dome and undergoing acinar to ductal transdifferentiation. CON, control; cKO, ERRγ cKO. All data are presented as mean ± SEM. * $p < 0.05$, *** $p < 0.005$, by student's t-test.

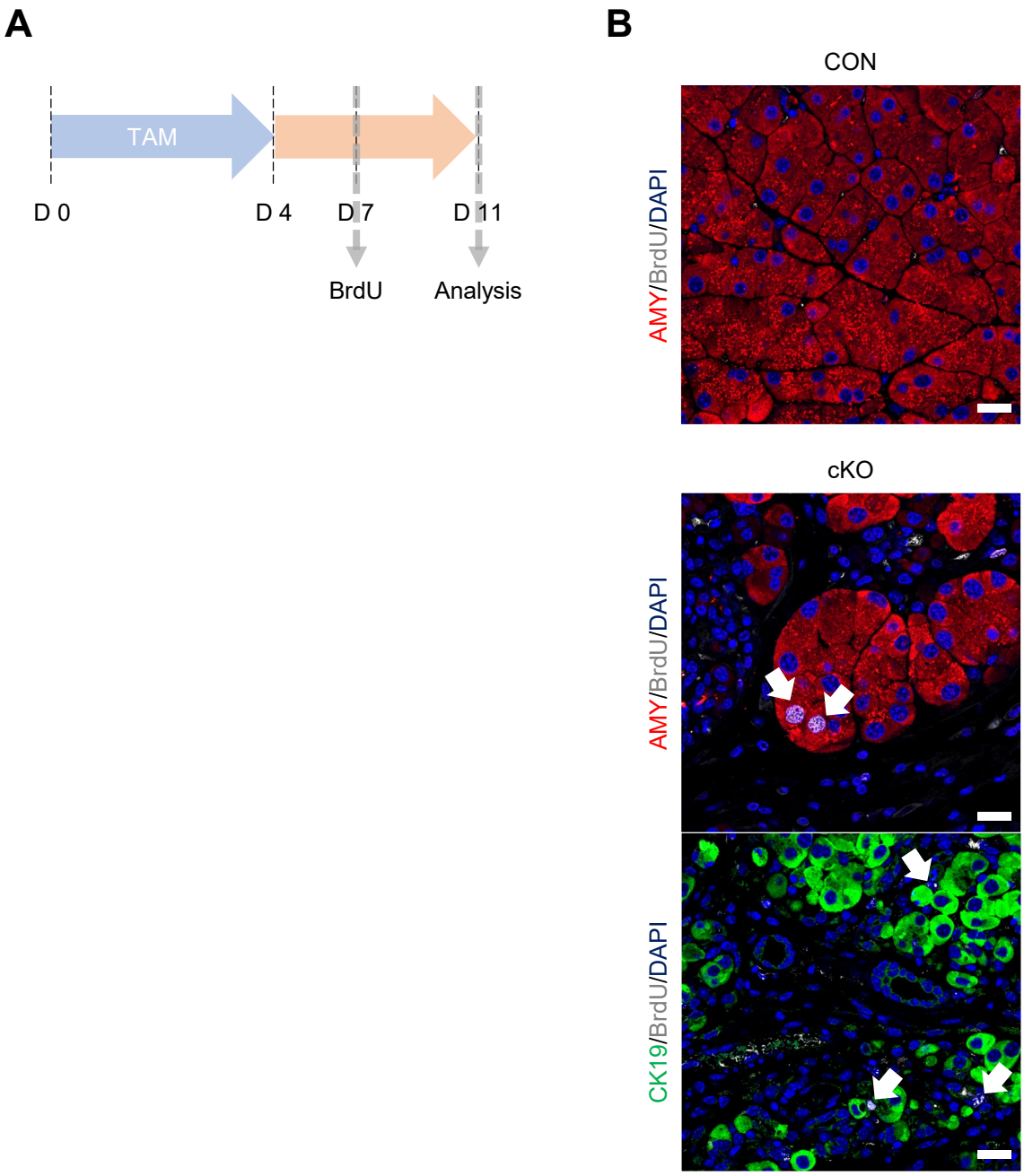

Supplementary Figure 13. Ductal cell proliferation is not a major contributor to the appearance of duct-like cells in ERRγ cKO pancreas.

(A) Scheme of experimental design for BrdU incorporation in control and ERRγ cKO mice. (B) Immunofluorescence staining of control and ERRγ cKO mice pancreas sections for amylase (AMY, red), BrdU (white) and DAPI (blue). CON, control; cKO, ERRγ cKO. Scale bar, 50 μm.

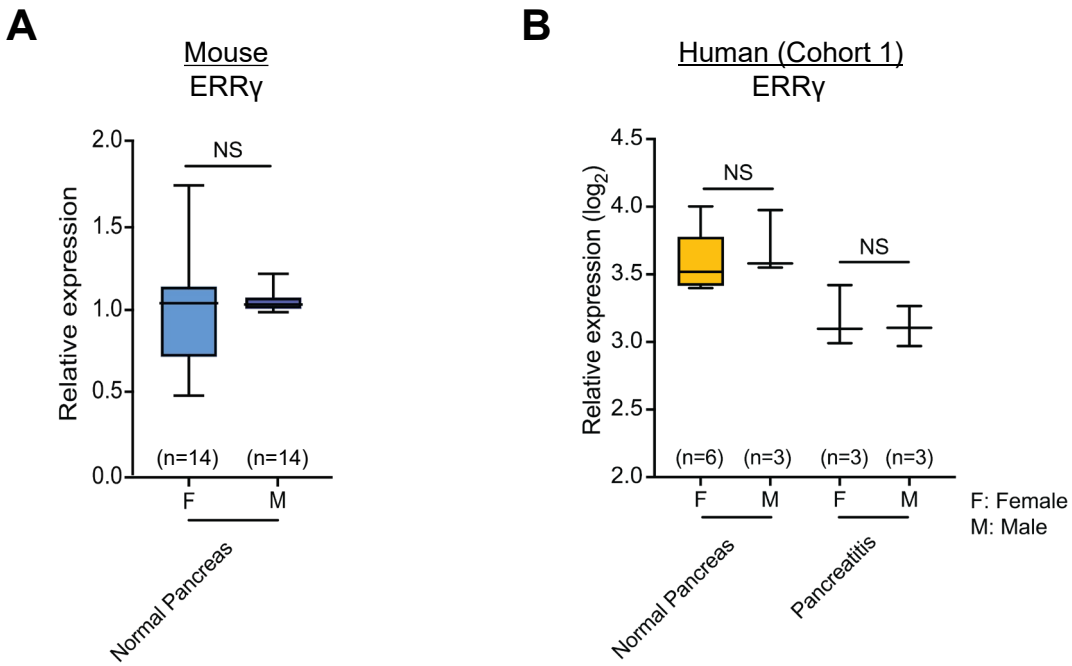

Supplementary Figure 14. ERRγ expression levels in the pancreas of male and female mice and human.

(A) ERRγ expression in normal pancreas from C57BL/6 mice (female, n =14; male, n = 14). (B) ERRγ expression in normal pancreas from normal (female, n = 6; male, n = 3) and pancreatitis (female, n = 3; male, n = 3) from human cohort 1 (GSE143754). The microarray data was extracted and normalized. Expression level shown as $\log_2$ scale.

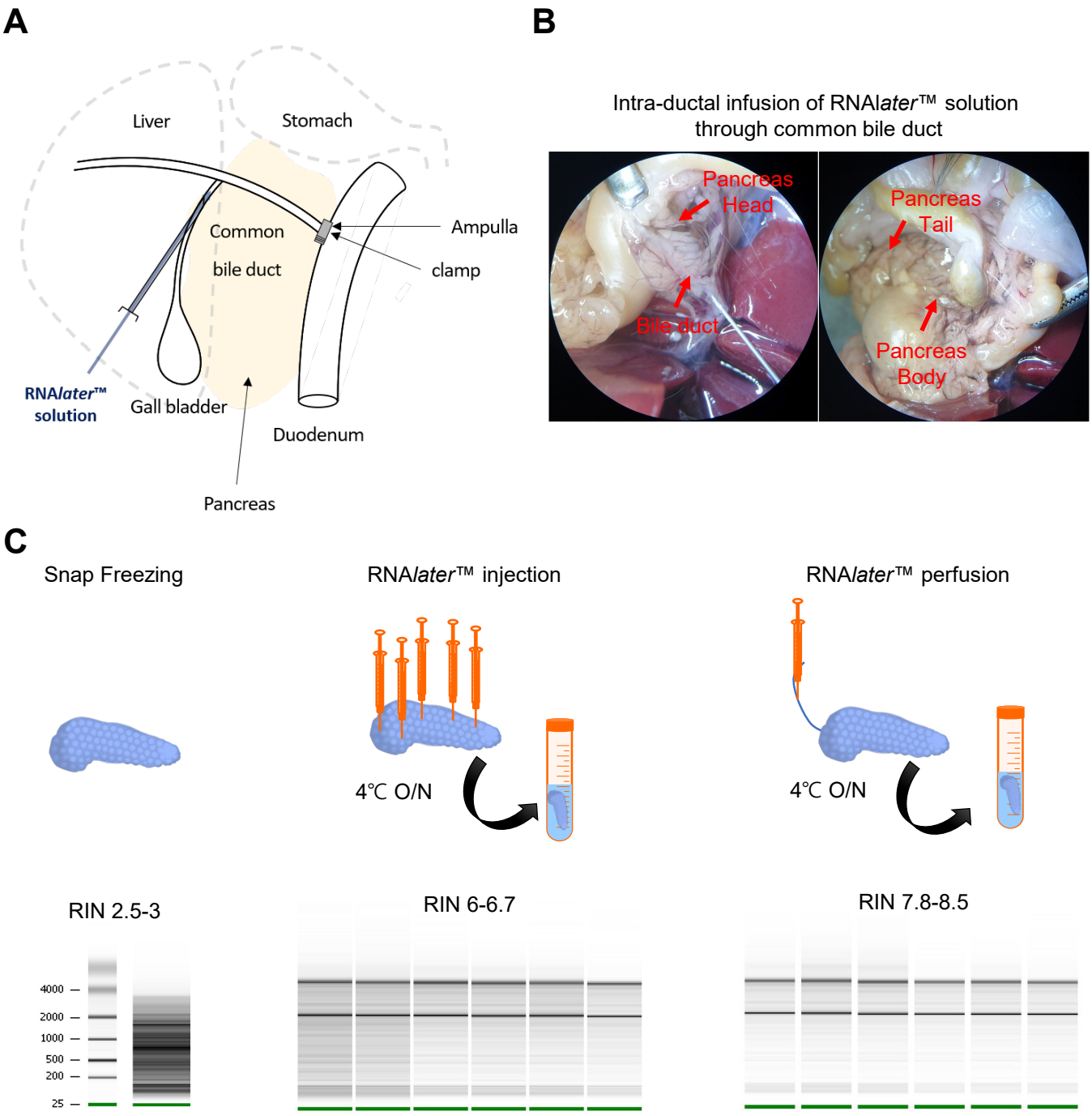

Supplementary Figure 15. High-quality RNA extraction procedure from pancreas.

(A) Illustration of intraductal infusion of RNA*later*™ solution into pancreas after ligation of common bile duct. (B) Images of intraductal infusion of RNA*later*™ solution into pancreas after ligation of common bile duct. (C) RNA integrity number (RIN) of RNA isolated from pancreas through three different methods

Metabolite	Concentration (ng/mg)		Normalized value[a]	Wilcoxon rank sum test
	CON	cKO		
Pyruvic acid	4.92 ± 1.10	5.13 ± 1.63	1.06	0.792
Lactic acid	385.00 ± 37.99	509.82 ± 68.40	1.32	0.017
Citric acid	35.15 ± 26.54	89.90 ± 22.54	3.82	0.004
cis-Aconitic acid	1.64 ± 0.99	3.50 ± 0.98	2.70	0.004
Isocitric acid	0.09 ± 0.08	0.26 ± 0.05	4.20	0.004
α-Ketoglutaric acid	4.42 ± 1.82	1.88 ± 0.58	0.40	0.009
2-Hydroxyglutaric acid	8.75 ± 1.23	7.76 ± 0.59	0.87	0.247
Succinic acid	7.24 ± 1.85	2.98 ± 1.03	0.39	0.004
Fumaric acid	31.08 ± 4.37	22.53 ± 3.33	0.70	0.004
Malic acid	79.36 ± 14.31	94.80 ± 12.36	1.23	0.126
Oxaloacetic acid	0.66 ± 0.03	0.63 ± 0.01	0.95	0.247
Glycolic acid	79.96 ± 11.28	111.25 ± 25.01	1.38	0.030
Acetoacetic acid	33.60 ± 42.19	128.95 ± 48.59	7.72	0.004
3-Hydroxybutyric acid	61.73 ± 18.07	69.61 ± 15.12	1.27	0.247
3-Hydroxyisobutyric acid	3.39 ± 1.49	3.73 ± 0.94	1.30	0.126
2-Hydroxybutyric acid	1.26 ± 0.75	2.11 ± 0.53	2.21	0.004
3-Hydroxypropionic acid	3.73 ± 0.33	5.35 ± 0.49	1.47	0.004
4-Hydroxyphenylacetic acid	0.35 ± 0.01	0.36 ± 0.02	1.03	0.329

[a] Values normalized to the corresponding control mean values

Supplementary Table 1. Levels of organic acids in pancreas tissues from control and ERRγ cKO mice.

Mice were intraperitoneally injected with tamoxifen (75 mg/kg) once daily for 5 consecutive days and sacrificed at day 4 after the final tamoxifen injection. Targeted metabolomics of organic acids from pancreas tissues were performed with MO/TBDMS derivatives by GC-MS/MS. CON, control (n = 5, male); cKO, ERRγ cKO (n = 5, male). Metabolite concentrations expressed as mean ± SD

Chr.	Position (GRCh37)	rs ID	Risk Allele	Other Allele	MAF	OR	P value
A. UKBB							
1	216756821	rs17669622	G	A	0.1343	0.82	0.00093
1	216819427	rs12023399	C	G	0.1517	0.81	0.00063
1	217303670	rs72743335	G	A	0.07	1.35	0.00079
1	217312568	rs201118685	CC	C	0.00007	0.82	9.80E-05
1	217324932	rs1502358	A	G	0.3142	0.82	0.00016
1	217318595	rs12119765*	T	C	0.4851	0.84	0.00040
B. NAPS2							
1	216527641	rs55720440	A	G	0.0196	0.33	0.0059
1	216731498	rs17668665	A	G	0.1633	0.71	0.0012
1	216989899	rs74899022	A	G	0.04613	1.93	0.0085
1	216998613	rs11117688	T	C	0.02566	0.54	0.0021
1	217014281	rs61817890	C	T	0.03055	0.55	0.0055
1	217090326	rs80280016	G	A	0.04277	1.54	0.0056
1	217092655	rs10779284	C	T	0.4685	0.81	0.0066

Supplementary Table 2. Genetic variants associated with regulatory elements within the *ESRRG* gene locus with an effect on chronic pancreatitis.

rs12119765* is the second highest single nucleotide variant (SNV) in the haplotype defined by rs76622060, since this SNV is reported to have a very low mutant allele fraction (MAF) in ALFA, but similar to rs12119765 in HaploReg. Chr., chromosome; Position on the chromosome; rsID, dbSNP reference number; MAF, minor allele frequency using the Allele Frequency Aggregator (ALFA) project allele frequency for Europeans; OR, odds ratio.

Chr.	Position (GRCh37)	rs ID	Risk Allele	Other Allele	MAF (ALFA EU)	OR	P value
UKBB AP							
1	216883643	rs2820879	C	T	0.1532	1.12	0.0034
1	216992598	rs115725121	G	A	0.00678	1.33	0.0034
1	217059291	rs17044247	C	T	0.1275	1.13	0.0027
1	217068430	rs76437375	T	C	0.01099	1.39	0.0016
1	217075587	rs61818569	T	G	0.01274	1.34	0.0039
1	217079179	rs61818570	G	A	0.01092	1.40	0.0016
1	217083207	rs17684269	T	C	0.1369	0.88	0.0074
1	217345024	rs116725108	G	T	0.01183	0.64	0.0078

Supplementary Table 3. Genetic variants associated with regulatory elements within the *ESRRG* gene locus with an effect on Acute pancreatitis.

The lead SNV was rs61818570 (OR = 1.40; p = 0.0016), which is linked to 5 intronic SNVs that alter gene promotor histone marks, enhancer histone marks, DNase susceptibility and multiple nucleotide binding site motifs based on HaploReg v4.1. Thus, there is a signal for an effect of alterations in *ESRRG* gene regulation in AP, but no SNV had strong statistical evidence (e.g. $p<0.01$, but not $p<0.001$).